

Strike-slip reactivation of segmented normal faults: implications for basin structure and fluid flow

A. Rotevatn* & D.C.P. Peacock

Department of Earth Science, University of Bergen, Allégaten 41, 5007 Bergen, Norway

*corresponding author: A. Rotevatn; atle.rotevatn@uib.no; phone: +4755583390

Abstract

Reverse reactivation of normal faults, also termed ‘inversion’, has been extensively studied, whereas little is known about the strike-slip reactivation of normal faults. At the same time, recognizing strike-slip reactivation of normal faults in sedimentary basins is critical, as it may alter and impact basin physiography, accommodation and sediment supply and dispersal. Motivated by this, we present a study of a reactivated normal fault zone in the Liassic limestones and shales of Somerset, UK, to elucidate the effects of strike-slip reactivation of normal faults, and the inherent deformation of relay zones that separate the original normal fault segments. The fault zone, initially extensional, exhibits a series of relay zones between right-stepping segments, with the steps between the segments having subsequently become contractional due to sinistral strike-slip movement. The relay zones have therefore been steepened and are cut by a series of connecting faults with reverse and strike-slip components. The studied fault zone, and comparison with larger-scale natural examples, lead us to conclude that the relays-turned-contractional-steps are associated with (i) complex fault and fracture networks that accommodate shortening, (ii) anomalously high numbers of fractures and faults, (iii) layer parallel slip and (iv) folding and uplift. Comparison with published statistics from global relay zones shows that whereas the reactivated relay

zones feature aspect ratios similar to those of unreactivated relay zones, bed dips within reactivated relay zones are significantly steeper than unreactivated relay zones. Given the potential of reactivated relay zones to form areas of local uplift, they may affect basin structure and may also form potential traps for hydrocarbon or other fluids. The elevated faulting and fracturing, on the other hand, means reactivated relays are also likely loci for enhanced up-fault flow.

Keywords: fault segmentation; relay zone; reactivation; strike-slip; restraining steps

1. Introduction

Normal fault systems are a critical element of extensional sedimentary basins, being the primary controls on basin boundaries, geometry, physiography, accommodation, sediment routing and fluid flow (e.g. Ebinger et al., 1993; Gawthorpe & Leeder, 2000; Henstra et al., 2016, 2017). Over the past several decades, there has been considerable research into the development of normal faults and extensional sedimentary basins (e.g. Anderson, 1951; Gibbs, 1984; Bosworth, 1985; Walsh & Watterson, 1987; Cartwright et al., 1995; Childs et al., 1995; Walsh et al. 2002, 2003; Jackson & Rotevatn, 2013; Rotevatn & Jackson, 2014; Jackson et al., 2017). This research has taught us that (i) normal fault systems are fundamentally and universally segmented (e.g. Peacock & Sanderson 1991; Cartwright et al., 1995; Hayward & Ebinger 1996; Peacock 2002; Walsh et al., 2003; Fossen & Rotevatn, 2016), and (ii) are associated with *transfer zones*, or *relay zones* (Fig. 1A-B), between stepping normal fault segments (e.g. Morley et al., 1990; Gawthorpe & Hurst, 1993; Peacock & Sanderson, 1994; Childs et al., 1995; Faulds & Varga, 1998; Rotevatn et al., 2007, 2009; Childs et al., 2017).

There has also been considerable interest in the reverse reactivation of normal fault systems (commonly termed “*positive inversion*”, or simply “*inversion*”; e.g. Buchanan & Buchanan, 1995; McClay 1989; Williams et al., 1989). The typical geometries that are produced during reverse reactivation of normal fault systems are therefore relatively well known from nature and experiments, including e.g. (i) inversion anticlines (e.g. Morley et al. 2003; Yamada & McClay 2004; Tavani et al., 2011); (ii) inversion thrust faults (e.g. McClay & Buchanan, 1992), (iii) thrust-ramps (e.g. McClay 1989), (iv) folding of the original fault(s) (e.g. Allen et al., 2001), and (v) uplift or upthrusting of hanging-wall wedges of syn-extensional “growth” strata (e.g. Roberts 1989; Panien et al., 2005). Although these are considered typical “inversion structures”, a wider range of geometries are possible during reverse reactivation of normal fault systems, depending on (i) the cross-sectional and along-strike geometry of the original normal fault system (e.g. Buchanan & McClay, 1991) and (ii) the timing and magnitude of reverse reactivation (e.g. McClay 1989; Brun & Nalpas, 1996).

There has, however, been very limited work on the *strike-slip* reactivation of normal faults (Fig. 1D-F), i.e. where a phase of normal-sense dip-parallel slip is succeeded by a reactivation phase of strike-parallel slip. Note that strike-slip reactivation of normal faults, where the slip vector during reactivation is parallel to the strike of the original normal fault, is different from both i) single-phase oblique extension (e.g. Clifton & Schlische, 2001; Brune et al., 2012), and ii) multi-phase extension where an initial orthogonal extension phase is succeeded by a phase of oblique extension on the first-phase faults (e.g. Henza et al., 2010; Henstra et al., 2015). Although strike-slip reactivation is reported in the literature (e.g. Hartz & Andresen, 1995; Kim, 1996; Aris et al., 1998; Balaguru et al., 2003; Faure et al., 2006; Ducea et al., 2009; Jankowski & Probulski, 2011; Turner et al., 2011; Firth et al., 2015), detailed descriptions of the strike-slip reactivation of normal faults (Van Noten et al., 2013) and the associated effects of reactivation on along-strike transfer zones (Barton et al., 1998;

Kelly et al., 1999; Zampieri & Massironi, 2007) are scarce. Thus, an understanding of key features and typical structures produced during strike-slip reactivation of normal faults is currently lacking.

Motivated by this, we here aim to elucidate the effects of strike-slip reactivation of normal faults, and the inherent effects on relay zones that separate normal fault segments. We also identify typical structures formed during strike-slip reactivation of normal faults, and the key geologic factors governing their formation. Furthermore, we discuss the possible effects of such reactivation on fluid flow along and around such faults, and how such reactivation may be identified on seismic data. Note that we separate between two separate scenarios when normal faults are reactivated in strike slip: When the reactivating strike-slip shear sense is identical to the stepping direction of the original extensional fault system (same-sense strike-slip reactivation), the original relay zones become extensional steps (e.g. right-lateral strike-slip reactivation of a right-stepping normal fault system). When the reactivating strike-slip shear sense is opposite to that of the stepping direction of the original extensional fault system (opposite-sense strike-slip reactivation), the original relay zones become contractional steps (e.g. left-lateral strike-slip reactivation of a right-stepping normal fault system). In this paper we focus on the latter scenario, i.e. reactivation of normal fault systems that turns relay ramps into contractional steps.

To address the above stated goals, we investigate a spectacularly well-exposed outcrop example of a normal fault zone (throw 8-20 m) reactivated in strike-slip in the Liassic limestones and shales at Lillstock on the Somerset coast, UK (Fig. 2), and discuss the findings in light of other, larger-scale examples. The fault zone exhibits a series of relay zones that separate right-stepping segments, with the steps between the segments having subsequently become contractional due to sinistral strike-slip reactivation (Fig. 1F). The fault zone was mapped using a base map constructed from merged photographs taken using an unmanned

aerial vehicle (*UAV* or *drone*) flown at ~ 20 m above the exposure. The merged image is available as supplementary material for this paper.

Understanding and recognizing strike-slip reactivation of normal faults in sedimentary basins is critically important since it may alter and influence the way in which faults control basin physiography, accommodation as well as sediment supply and dispersal (see e.g. Kristensen et al., 2018). Furthermore, the results of this work has economic implications, since advances in the understanding of normal faults reactivated in strike-slip may lead to improvements of our understanding of fluid flow, fluid retention and leakage, and trap-forming mechanisms relevant for e.g. petroleum exploration, subsurface carbon storage, groundwater aquifer management and extraction of geothermal energy.

2. Terminology

The terminology used in this paper is defined in Peacock et al. (2000, 2016) and Biddle & Christie-Blick (1985), with Figure 1 illustrating some of the geometries described. While *transfer zone* is used by Dahlstrom (1970) for the structures that conserve shortening, or allow a regular change in shortening, between overstepping thrust faults, the term is generally used for an area of deformation and bed rotation between two normal faults that overstep in map view (e.g. Morley, 1995). Morley et al. (1990, their Fig. 1) describe *synthetic transfer zones* and *conjugate transfer zones*, in which the overstepping faults dip in the same and opposite directions respectively (Fig. 1A). A *relay ramp* (*synthetic transfer zone* of Morley et al., 1990) is an area of reoriented bedding between two normal faults that overstep in map view and that have the same dip direction (Fig. 1B; e.g. Larsen, 1988; Peacock & Sanderson, 1991; Huggins et al., 1995). If a relay ramp is breached by one or more *connecting faults* (Fig. 1C), it is termed a *breached relay*. The term *relay zone* encompasses both relay ramps (Fig. 1B) and breached relays (Fig. 1C; e.g. Peacock et al., 2016).

3. Outcrop example of a normal fault zone reactivated in strike-slip at Lillstock, Somerset, UK

3.1. Geological background

Mapping has been carried out on a fault zone on Lillstock Beach, Somerset, UK (Figs. 2 and 3). The fault zone occurs in wavecut platform exposures of Liassic limestones and shales (e.g. Whittaker & Green, 1983). Peacock & Sanderson (1999) show that the deformation at Lillstock involves the following:

1. 060° striking veins, and possibly normal faults, are locally developed and indicate approximate 150°-330° extension.
2. Normal faults and calcite veins strike at about 095° and indicate approximate north-south extension. Oblique fibres in the veins indicate sinistral transtension, consistent with NNW-SSE-directed extension. This event may be consistent with approximate NW-SE extension in the Wessex Basin from the Permian to the Cretaceous, described by Chadwick (1986) and by Lake & Karner (1987). Nucleation, growth and normal slip on the studied fault system can likely be attributed to this stage of deformation.
3. Approximate east-west contraction is indicated by conjugate arrays of veins and pull-aparts (described by Peacock & Sanderson, 1995), and by sinistral shear on some of the 095° striking normal faults. Sinistral reactivation of the studied fault system is likely related to this stage of deformation.
4. Dextral reactivation occurred on some of the 095° striking normal faults. Calcite veins developed striking at approximately 150°, with reactivation of some 100° striking veins. Van Hoorn (1987) describes late Jurassic to early Cretaceous dextral strike-slip movement

on east-west structures further west in the Bristol Channel Basin.

5. Approximate north-south contraction is indicated by east-west thrusts, strike-slip faults conjugate about north-south, veins striking approximately north-south, and by east-west striking stylolites. This event is probably related to contraction during the Alpine Orogeny (Dart et al., 1995). Approximate north-south contraction during the late Cretaceous to middle Tertiary is also described in the Wessex Basin by Chadwick (1993).
6. The joints post-date the faulting events, because the joints abut the faults and they are not mineral-filled (Rawnsley et al., 1998).

3.2. Present-day fault geometry and segmentation

The Liassic of Somerset consists of a sequence of limestone and shale beds (e.g. Whittaker & Green, 1983), the thicknesses of which may be used to identify the separation between originally adjoined points or horizons in the hanging-wall and footwall of a fault, and thereby to measure the displacement, throw or heave (e.g. Kelly et al., 1999). The studied fault zone at Lilstock is E-striking, S-dipping, and is exposed for ~ 310 m along strike, with the eastern end in the cliff and the western end disappearing under a cover of sand (Fig. 3A). The exposed fault zone is comprised of five main right-stepping segments from east to west (Fig. 3A): (i) **Segment A** is poorly-exposed (and thus not shown in Fig. 3A) over a few metres and terminates eastward into a cliff; (ii) **Segment B** also terminates eastwards immediately before the same cliff and is poorly-exposed over a distance of ~ 74 m; (iii) **Segment C** is ~ 110 m long and its western end is well-exposed; (iv) **Segment D** is ~ 74 m long and is well-exposed along its entire length; (v) **Segment E** is well-exposed over ~ 95 m, but disappears under a cover of sand to the west.

All of segments A through E are separated by steeply dipping breached relays (Fig. 3A), which we from here on will refer to as relay zones. Fault segments A and B are separated by a

174 relay zone with a length (fault overlap) of 30 m, maximum width (distance between the two
175 bounding faults) 10 m, and a maximum dip of relay bedding of 33°. The relay zone separating
176 fault segments B and C (Fig. 3A) is 31 m long and up to 8 m wide, with a maximum relay bed
177 dip of 41°. The best exposed relay zone (Fig. 3B) separates segments C and D and is
178 approximately 58 m long, with a width of up to 11 m; bedding within the relay zone exhibits a
179 maximum dip of 48°. Fault segments D and E are separated by a relay zone (Fig. 3A) with
180 length 68 m, maximum width 12 m, and maximum relay bed dips of 39°.

181 Whereas relay zones in extensional fault systems typically feature a down-stepping
182 relief-reducing geometry, the relay zones in the study area exhibit some positive relief and
183 therefore are localised structural highs in the studied fault system (Fig. 4A and B). Internally,
184 the ramps are characterised by: (i) steepening of the bedding to dips of up to approximately
185 45° (Fig. 4B); (ii) strike-slip faults that are antithetic to the strike-slip displacement on the
186 reactivated normal faults (Fig. 3B); (iii) strike-slip faults that are synthetic to the strike-slip
187 displacement on the reactivated normal faults; (iv) calcite veins indicating sinistral
188 transtension (Fig. 4C); (v) locally-developed fold-thrust structures (Fig. 4E), (vi) layer-
189 parallel slip (Fig. 4E), and; (e) locally-developed crenulation cleavage in shale beds (Fig. 4F).

191 *3.3. Evidence for normal slip and subsequent strike-slip reactivation*

192 Stratigraphic cross-fault correlation suggests a net throw of between ~ 8 m and ~ 20 m
193 down to the south, showing that the fault has a normal displacement. Other evidence for
194 normal displacement includes E-W striking calcite veins and normal faults in the footwall
195 (Fig. 5).

196 The initial observation that led us to hypothesize that the fault system had been
197 reactivated in strike-slip was that the relay zones between the right-stepping segments
198 appeared over-steepened (Figs. 3B and 4A). In fact, the relay zones are much steeper than is

typical of relay zones in Liassic rocks elsewhere on the Somerset coast, and for relay zones in general (e.g. Peacock & Sanderson 1991, 1994; Fossen & Rotevatn 2016; see Section 5 for full discussion). We thus tentatively interpreted the steep relay zone dips as a result of local contraction due to sinistral strike-slip reactivation of the normal fault system (see Fig. 1F).

The following lines of evidence offer independent support for strike-slip reactivation:

(i) fault lineations (slickensides) indicate approximate strike-slip displacements (Fig. 4C).

(ii) left-stepping vein arrays that strike approximately E-W in the walls of the fault zone also indicate sinistral strike-slip deformation (Fig. 4B)

(iii) the network of faults and other structures within the steepened relay zones (Fig. 3B and 6A) also indicates contractional deformation, including fold-thrust structures (Fig. 4E) and crenulation cleavage (Fig. 4F). Localized contraction within the relay zones is consistent with sinistral strike-slip reactivation.

Reliable offset markers to determine the magnitude of strike-slip displacement are scarce or absent; however, based on the sum of field observations we estimate that strike-slip displacement falls in the range of 1-5 m.

4. Discussion

4.1 Typical geometries and effects associated with of strike-slip reactivation of normal faults

Strike-slip reactivation of normal fault zones mean that any irregularity along that original fault zone will take on a new role as a locus for localised (oblique) contraction or extension. The highest-order and most prominent irregularities in the along-strike geometry of a segmented normal fault zone are the relay zones that separate adjacent segments. In the following we discuss the field observations made herein and draw parallels to published larger-scale examples and scaling relations, to draw out typical effects and geometries

associated with strike-slip reactivation of normal faults, and particularly the effect of reactivation of relay zones. In the case of the example presented in Fig. 3, where a right-stepping normal fault zone is reactivated as a sinistral strike-slip fault, such relay zones become sites of localised contraction (as would the dextral strike-slip reactivation of a left-stepping normal fault system) (Fig. 6). This, being the case-in-point, will form the main focus for the discussion.

Relay zones in normal fault systems are generally known to be zones of high fault (and commonly other fracture type) intensity and connectivity (e.g. Rotevatn et al., 2007; Bastesen & Rotevatn, 2012; Dimmen et al., 2017), as well as a wide variety of fault orientations due to fault interaction and stress perturbation in the relay zones (e.g. Crider & Pollard, 1998; Kattenhorn et al., 2000). This is the reason why relay zones are often described as areas of enhanced structural “complexity”. When such relay zones are subjected to a second phase of deformation during strike-slip reactivation, such structural “complexity” is bound to increase as new structures grow within the relay zones. Within the relay zones of the fault zone studied herein, growth of structures formed during strike-slip reactivation (intra-ramp strike-slip faults and thrusts) have led to higher total fault intensities and connectivity than what would have been the case prior to fault reactivation. This finds support also in larger-scale examples; for example, Peacock & Shepherd (1997) describe km-scale faults in the Sydney Basin, Australia. They show that relay zones in a right-stepping normal fault system reactivated in sinistral strike-slip were characterised by sinistral strike-slip faults and thrusts within the relay zones, and concluded that the complex patterns of deformation typically seen in relay zones and transfer zones were generally increased during (strike-slip) reactivation.

Whereas the internal structure of relay zones in normal fault systems is generally dominated by normal-slip faults and extension fractures, the reactivated relay zones shown herein also feature thrust faults and strike-slip faults. This is supported by similar finds in

other studies (Peacock & Shepherd, 1997; Zampieri & Massironi, 2007); Zampieri & Massironi (2007) also show that (strike-slip) reactivated relay zones are typified by inversion of pre-existing normal faults and layer-parallel faulting.

Relay zones are also known to be associated with gentle, monoclinal folding of relay beds (e.g. Larsen 1988; Peacock & Sanderson, 1991, 1994; Fossen & Rotevatn, 2016). In the relay zones of the herein studied fault system, the relay zones have steeper dips than are typical of other relay zones in the area. Also, they include local development of fold-thrust structures (Fig. 4E) and crenulation cleavage (Fig. 4F). Similarly, in a study of a km-scale similarly reactivated fault system in the Italian Alps, Zampieri & Massironi (2007) show that relay zones are associated with increased and higher-amplitude folding compared to non-reactivated relay zones (Fig. 7).

The relay zones in the studied fault systems represent local structural highs. While relay zones in extensional fault systems represent a downward stair-stepping structure from the footwall to the hangingwall (e.g. Larsen, 1988; Peacock & Sanderson 1991, 1994), localised shortening of the relay zones means they may form local structural highs along strike of the reactivated fault system. The localised shortening is responsible for a tendency to turn the former relay zones into positive structures due to folding, tilting and thrusting, much like is seen at restraining bends and steps along primary strike-slip faults (e.g. Sylvester, 1988; McClay & Bonora, 2001; Cunningham & Mann, 2007; Dooley & Scheurs, 2012). On the plate-boundary scale, a relevant example for comparison is the Sulaiman-Kirthar arcuate fold-thrust belt in Pakistan (Fig. 8). This originated as a 100s-km-scale transfer zone in a Mesozoic rift system between Africa, Madagascar and India (e.g. Scotese, 1991; Haq & Davis, 1997), but underwent sinistral reactivation in Eocene times during the collision between the Indian and Eurasian plates (Dewey et al., 1989; Haq & Davis, 1997), leading the transfer zone to turn into an arcuate fold and thrust belt (Fig. 8).

4.2 Scaling relations and bed dips of reactivated relay zones compared to un-activated relay zones

The relay zones in this study show similar relationships between relay length (fault overlap) and relay width (fault separation) as do relay zones in non-activated normal fault systems. This is shown in Figure 9, where the four reactivated relay zones studied herein show similar aspect ratios as relay zones in normal fault systems globally (see also Mansfield & Cartwright, 2001, Long & Imber, 2011, Fossen & Rotevatn, 2016). As such, aspect ratio appear not to be distinctive for reactivated relay zones when compared to non-activated relay zones.

The relay bed dips, however, are much steeper than is typical of relay zones in Liassic rocks elsewhere on the Somerset coast, and for relay zones in general. For example, Peacock & Sanderson (1991, 1994) show relay zones in the study area between stepping normal faults with dips of up to about only 20°. Figure 10 shows a comparison of the relay zone steepness data from this study and data from Fossen & Rotevatn (2016), who show, based on global outcrop-based data (from Soliva & Benedicto, 2004; Huggins et al., 1995; Xu et al., 2011; Giba et al., 2012; Bastesen & Rotevatn, 2012; Rotevatn & Bastesen, 2014) that unbreached, partly breached and fully breached relay zones have mean bed dips of 7°, 13° and 18°, respectively (the maximum dip reported was for a breached relay, at 32°). The relay zones in the fault zones at Lillstock, however, shows dips of up to about 48° (Figs. 3, 4A and 10). This suggests that relay zone dips higher than 20-30° is atypical for relay zones in normal fault systems, and that relay bed dips in excess of 30-35° is probably diagnostic of relay zones that have been shortened and thus over-steepened. Note that continued strike-slip would likely lead to relay abandonment at some point, after which relay steepening and internal deformation would largely cease. Further studies of other natural examples, or physical

analogue experiments, of normal faults reactivated in larger-magnitude strike-slip (e.g. greater than the original normal-sense slip) would be needed to further investigate this.

4.3 Implications for fluid flow in sedimentary basins

The main implications for fluid flow in normal fault systems reactivated in strike-slip, where relay zones become zones of localised shortening, may be summarised in two points: Firstly, the relay zones are associated with high fault intensities that are amplified by the strike-slip fault reactivation, which means that the number and connectivity of faults and related fractures in reactivated relay zones are anomalously high. It is therefore likely that reactivated relay zones represent along-strike loci for enhanced up-fault fluid flow (cf. Fossen et al., 2010; Rotevatn & Bastesen, 2014; Peacock et al., 2017). Numerous studies have shown similar effects of structural complexity on the loci of fluid flow in non-reactivated normal fault systems (e.g. Davatzes & Aydin, 2003; Gartrell et al., 2004; Dockrill & Shipton, 2010). For example, Rowland & Sibson (2004) show that steps and transfer zones in a segmented rift system in New Zealand are associated with a concentration of geothermal fields, which they relate to locally-enhanced vertical permeability in such zones. Secondly, the reactivated relay zones may represent local structural highs along strike, which means that such locations are associated with structural trap formation where fluids, such as hydrocarbons, may potentially accumulate (cf. Fossen et al., 2010).

4.4 Diagnostics of strike-slip reactivation of normal faults from seismic reflection data

Evidence from seismic reflection data is commonly used to identify reverse reactivation of normal faults, including reverse displacements higher up the fault and forced folds above the fault (e.g. Coward, 1996). In contrast, the scarcity of accounts of the strike-slip reactivation of normal faults suggests either that (i) strike-slip reactivation of normal faults is

uncommon, or (ii) that evidence for reactivation may be subtler than structures created by reverse reactivation. There is no evidence-based reason to suspect the former, and given the known challenges associated with the imaging of strike-slip dominated systems from seismic reflection data (McClay & Bonora, 2001), the under-reporting is likely related to difficulties of recognizing strike-slip reactivation from seismic data.

We suggest that the following should be taken as suggestive of strike-slip reactivation when investigating normal fault systems using seismic reflection data:

Clear seismic evidence of normal offset, as well as one or more of the following:

- Seismically identifiable strike-slip offset, although this is generally difficult to pinpoint from seismic reflection data.
- Inversion only of selected faults, particularly at or near relay zones or fault bends
- Relay beds steeper than 30-35° (see Section 5.2 and Fig. 10).
- Areas of uplift (folds, thrust-related features) at relay zones and/or fault bends.
- Evidence for contractional deformation at relay zones.
- Network of faults, within and around relay zones, that accommodate shortening.

4.5 Releasing strike-slip reactivation of normal fault zones

Although the current study focuses on an example where relay zones are turned into sites of localised contraction during strike-slip reactivation, localised extension of the original relay zones may also occur. This would be the case where a right-stepping normal fault system is reactivated in dextral strike-slip, or where sinistral reactivation affects a left-stepping normal fault system. Here, relay zones may turn into areas of localised subsidence, or pull-apart basins, as the transfer zones along normal faults become reactivated as extensional steps by strike-slip deformation (e.g. Richard and Krantz, 1991; Wong and

Munguía, 2006; Zampieri and Massironi, 2007). This style of strike-slip reactivation of normal faults has not been the focus of this study but will form the focus of future work.

5. Summary and conclusions

This paper has aimed to elucidate the phenomenon of strike-slip reactivation of segmented normal faults, and specifically opposite-sense strike slip-reactivation, i.e. the scenario when the strike-slip reactivation sense of shear (right-or-left-lateral) is the opposite of the stepping direction of the original fault system (as in this case, left-lateral strike-slip reactivation of a right-stepping normal fault).

During opposite-sense strike-slip reactivation of a stepping, segmented normal fault zone, the relay zones of the original normal fault system are reactivated as contractional steps, leading to shortening and over-steepening of the relay zones. We reach the following conclusions regarding the overall geometry and structure of the reactivated relays:

- Reactivated relay zones are affected internally by thrusts and strike-slip faults that overprint pre-existing extensional structures.
- Complex fault (and other fracture) networks accommodate shortening within the relay zones. The relay zones are therefore typified by anomalously high numbers of fractures and faults, and high fault- and fracture connectivities.
- Layer parallel slip accommodating shortening is common.
- The reactivated relay zones are associated with more folding of relay beds, and may feature anticlines rather than the monoclines that typify relays unaffected by reactivation.
- The reactivated relay zones feature aspect ratios similar to those of relay zones that have not been reactivated.

- Due to shortening and associated tilting, bed dips within reactivated relays are significantly steeper than relay zones in unreactivated normal fault systems. The shortening may also lead to localized uplift at the relays-turned-contractional-steps.

Recognizing strike-slip reactivation of normal fault zones in sedimentary basins may be crucial, as modification of relay zones and the reconfiguration of structural highs and lows along-strike has implications for basin physiography, accommodation, sediment supply and dispersal (see e.g. Kristensen et al., 2018). Furthermore, given their potential to form localized uplifts, relays reactivated as contractional steps may form potential traps for hydrocarbons or other fluids. Conversely, the increased fracturing at reactivated relays may increase the risk of leakage, and means they are likely sites of localized, enhanced up-fault fluid flow. As such they may form loci for geothermal upwelling, ore mineral deposits and fluid rock interactive processes in general.

Conflicts of interest

A. Rotevatn is an Associate Editor in Basin Research.

Acknowledgements

This is a preprint version of a paper published in Basin Research (<http://dx.doi.org/10.1111/bre.12303>). BKK is thanked for funding D.C.P. Peacock's time on this project through a grant in context of the BKK-UiB agreement. We also acknowledge financial support for the ANIGMA project from the Research Council of Norway (project no. 244129/E20) through the ENERGIX program, and from Statoil ASA through the Akademia

agreement. Comments from John Conneally and Mark Swanson helped improved the quality of this preprint.

References

ANDERSON, E.M. (1951) The Dynamics of Faulting. Oliver and Boyd, Edinburgh.

ALLEN, M.B., ALSOP, G.I., ZHEMCHUZHNIKOV, V.G. (2001) Dome and basin refolding and transpressive inversion along the Karatau Fault System, southern Kazakhstan. *Journal of the Geological Society*, 158, 83-95.

ARIS, Y., COIFFAIT, P.E., GUIRAUD, M. (1998) Characterisation of Mesozoic–Cenozoic deformations and palaeostress fields in the Central Constantinois, northeast Algeria. *Tectonophysics*, 290, 59-85.

BALAGURU, A., NICHOLS, G., HALL, R. (2003) The origins of ‘circular basins’ of Sabah, Malaysia. *Geological Society of Malaysia*, 46, 335-351.

BARTON, C.M., EVANS, D.J., BRISTOW, C.R., FRESHNEY, E.C., KIRBY, G.A. (1998) Reactivation of relay zones and structural evolution of the Mere Fault and Wardour Monocline, northern Wessex Basin. *Geological Magazine*, 135, 383-395.

BASTESEN, E., ROTEVATN, A. (2012) Evolution and structural style of relay zones in layered limestone–shale sequences: insights from the Hammam Faraun Fault Block, Suez rift, Egypt. *Journal of the Geological Society*, 169, 477-488.

BIDDLE, K.T. AND CHRISTIE-BLICK, N. (1985). Glossary—strike-slip deformation, basin formation, and sedimentation. *SEPM Special Publications* 37, 375-384.

BOSWORTH, W. (1985) Geometry of propagating continental rifts. *Nature* 316, 625-627.

BRUN, J.P., NALPAS, T. (1996) Graben inversion in nature and experiments. *Tectonics*, 15, 677-687.

- 419 BRUNE, S., POPOV, A. A., SOBOLEV, S. V. (2012) Modeling suggests that oblique
 420 extension facilitates rifting and continental break-up. *Journal of Geophysical Research:*
 421 *Solid Earth*, 117(B8).
- 422 BUCHANAN, J.G., BUCHANAN, P.G. (eds.) (1995) Basin Inversion. *Geological Society*
 423 *Special Publication* 88.
- 424 BUCHANAN, P.G., MCCLAY, K.R. (1991) Sandbox experiments of inverted listric and
 425 planar fault systems. *Tectonophysics*, 188, 97-115.
- 426 CARTWRIGHT, J.A., TRUDGILL, B.D., MANSFIELD, C.S. (1995) Fault growth by
 427 segment linkage: an explanation for scatter in maximum displacement and trace length
 428 data from the Canyonlands Grabens of SE Utah. *Journal of Structural Geology*, 17,
 429 1319-1326.
- 430 CHADWICK, R.A. (1986) Extension tectonics in the Wessex Basin, southern England.
 431 *Journal of the Geological Society, London*, 143, 444-465.
- 432 CHADWICK, R.A. (1993) Aspects of basin inversion in southern Britain. *Journal of the*
 433 *Geological Society, London*, 150, 311-322.
- 434 CHILDS, C., MANZOCCHI, T., NICOL, A., WALSH, J. J., SODEN, A. M., CONNEALLY,
 435 J. C., & DELOGKOS, E. (2017) The relationship between normal drag, relay ramp
 436 aspect ratio and fault zone structure. *Geological Society, London, Special Publications*,
 437 439, 355-372.
- 438 CHILDS, C., WATTERSON, J., WALSH, J.J. (1995) Fault overlap zones within developing
 439 normal fault systems, *Journal of the Geological Society, London*, 152, 535-549.
- 440 CLIFTON, A.E., SCHLISCHE, R.W. (2001) Nucleation, growth and linkage of faults in
 441 oblique rift zones: results from experimental clay models and implications for maximum fault
 442 size. *Geology*, 29, 455-458.

- 443 COWARD, M.P. (1996) Balancing sections through inverted basins. In: Buchanan, P.G.,
444 Nieuwland, D.A. (eds.), Modern Developments in Structural Interpretation, Validation
445 and Modelling. *Geological Society, London, Special Publications*, 99, 51-77.
- 446 CRIDER, J.G. AND POLLARD, D.D. (1998) Fault linkage: Three-dimensional mechanical
447 interaction between echelon normal faults. *Journal of Geophysical Research: Solid*
448 *Earth*, 103 (B10), 24373-24391.
- 449 CUNNINGHAM, W.D. AND MANN, P. (2007) Tectonics of strike-slip restraining and
450 releasing bends. *Geological Society, London, Special Publications*, 290, 1-12.
- 451 DAHLSTROM, C.D.A. (1970). Structural geology in the eastern margin of the Canadian
452 Rocky Mountains. *Bulletin Canadian Petroleum Geology*, 18, 332-406.
- 453 DART, C.J., MCCLAY, K., HOLLINGS, P.N. (1995) 3D analysis of inverted extensional
454 fault systems, southern Bristol Channel basin, U.K. In Buchanan, J.G., Buchanan, P.G.
455 (eds.) Basin Inversion. *Geological Society, London, Special Publications*, 88, 393-413.
- 456 DAVATZES, N.C. AND AYDIN, A. (2003) Overprinting faulting mechanisms in high
457 porosity sandstones of SE Utah. *Journal of Structural Geology*, 25, pp.1795-1813.
- 458 DEWEY, J., CANDE, S. AND PITMAN, W.C.I.I.I. (1989) The tectonic evolution of the
459 India/Eurasia collision zone. *Ecolgae Geologicae Helvetiae*, 82, 717-734.
- 460 DOCKRILL, B. AND SHIPTON, Z.K. (2010) Structural controls on leakage from a natural
461 CO₂ geologic storage site: Central Utah, USA. *Journal of Structural Geology*, 32,
462 1768-1782.
- 463 DIMMEN, V., ROTEVATN, A., PEACOCK, D.C., NIXON, C.W. AND NÆRLAND, K.
464 (2017) Quantifying structural controls on fluid flow: Insights from carbonate-hosted
465 fault damage zones on the Maltese Islands. *Journal of Structural Geology*, 101, 43-57.
- 466 DOOLEY, T.P. AND SCHREURS, G. (2012) Analogue modelling of intraplate strike-slip
467 tectonics: A review and new experimental results. *Tectonophysics* 574, 1-71.

- 468 DUCEA, M.N., KIDDER, S., CHESLEY, J.T., SALEEBY, J.B. (2009) Tectonic underplating
469 of trench sediments beneath magmatic arcs: the central California example.
470 *International Geology Review*, 51, 1-26.
- 471 EBINGER, C. J., DEINO, A. L., TESSA, A. L., BECKER, T., RING, U. (1993). Tectonic
472 controls on rift basin morphology: evolution of the Northern Malawi (Nyasa) Rift.
473 *Journal of Geophysical Research: Solid Earth*, 98(B10), 17821-17836.
- 474 ENGELDER, T., PEACOCK, D. C. P. (2001). Joint development normal to regional
475 compression during flexural-flow folding: the Lilstock buttress anticline, Somerset,
476 England. *Journal of Structural Geology*, 23, 259-277.
- 477 FAULDS, J.E., VARGA, R.J. (1998) The role of accommodation zones and transfer zones in
478 the regional segmentation of extended terranes. In: Faults, J.E., Stewart, J.H., (eds.),
479 Accommodation zones and transfer zones: the regional segmentation of the Basin and
480 Range Province. *Geological Society of America Special Publication*, 323, pp. 1-45.
- 481 FAURE, S., TREMBLAY, A., MALO, M., ANGELIER, J. (2006) Paleostress analysis of
482 Atlantic crustal extension in the Quebec Appalachians. *The Journal of Geology*, 114,
483 435-448.
- 484 FIRTH, E.A., HOLWELL, D.A., OLIVER, N.H.S., MORTENSEN, J.K., ROVARDI, M.P.,
485 BOYCE, A.J. (2015) Constraints on the development of orogenic style gold
486 mineralisation at Mineral de Talca, Coastal Range, central Chile: evidence from a
487 combined structural, mineralogical, S and Pb isotope and geochronological study.
488 *Mineralium Deposita*, 50, 675-696.
- 489 FOSSEN, H., ROTEVATN, A. (2016) Fault linkage and relay structures in extensional
490 settings – a review. *Earth-Science Reviews*, 154, 14-28.
- 491 FOSSEN, H., SCHULTZ, R.A., RUNDHOVDE, E., ROTEVATN, A. AND BUCKLEY, S.J.
492 (2010) Fault linkage and graben stepovers in the Canyonlands (Utah) and the North Sea

- 493 Viking Graben, with implications for hydrocarbon migration and accumulation. *AAPG*
494 *Bulletin*, 94, 597-613.
- 495 GARTRELL, A., ZHANG, Y., LISK, M. AND DEWHURST, D. (2004) Fault intersections
496 as critical hydrocarbon leakage zones: integrated field study and numerical modelling of
497 an example from the Timor Sea, Australia. *Marine and Petroleum Geology*, 21, 1165-
498 1179.
- 499 GAWTHORPE, R.L., HURST, J.M. (1993) Transfer zones in extensional basins: their
500 structural style and influence on drainage development and stratigraphy. *Journal of the*
501 *Geological Society, London*, 150, 1137-1152.
- 502 GAWTHORPE, R. L., LEEDER, M. R. (2000). Tectono-sedimentary evolution of active
503 extensional basins. *Basin Research* 12, 195-218.
- 504 GIBA, M., WALSH, J.J., NICOL, A. (2012) Segmentation and growth of an obliquely
505 reactivated normal fault. *Journal of Structural Geology*, 39, 253-267.
- 506 GIBBS, A. D., 1984. Structural evolution of extensional basin margins. *Journal of the*
507 *Geological Society of London*, 141, 609-620.
- 508 HAQ, S.S. AND DAVIS, D.M. (1997) Oblique convergence and the lobate mountain belts of
509 western Pakistan. *Geology*, 25, 23-26.
- 510 HARTZ, E., ANDRESEN, A. (1995) Caledonian sole thrust of central East Greenland: a
511 crustal-scale Devonian extensional detachment? *Geology*, 23, 637-640.
- 512 HAYWARD, N., EBINGER, C. (1996) Variations in the along-axis segmentation of the Afar
513 Rift system. *Tectonics*, 15, 244-257.
- 514 HENZA, A.A., WITHJACK, M.O. AND SCHLISCHE, R.W. (2010) Normal-fault
515 development during two phases of non-coaxial extension: An experimental study.
516 *Journal of Structural Geology*, 32, 1656-1667.

- 517 HENSTRA, G.A., GAWTHORPE, R.L., HELLAND-HANSEN, W., RAVNÅS, R.,
 518 ROTEVATN, A. (2017). Depositional systems in multiphase rifts: seismic case study
 519 from the Lofoten margin, Norway. *Basin Research* 29, 447-469.
- 520 HENSTRA, G.A., GRUNDEVÅG, S.A., JOHANNESSEN, E.P., KRISTENSEN, T.B.,
 521 MIDTKANDAL, I., NYSTUEN, J.P., ROTEVATN, A., SURLYK, F., SÆTHER, T.,
 522 WINDELSTAD, J. (2016) Depositional processes and stratigraphic architecture within
 523 a coarse-grained rift-margin turbidite system: The Wollaston Forland Group, east
 524 Greenland. *Marine and Petroleum Geology*, 76, 187-209.
- 525 HENSTRA, G.A., ROTEVATN, A., GAWTHORPE, R.L. AND RAVNÅS, R. (2015)
 526 Evolution of a major segmented normal fault during multiphase rifting: The origin of
 527 plan-view zigzag geometry. *Journal of Structural Geology*, 74, 45-63.
- 528 HUGGINS, P., WATTERSON, J., WALSH, J.J., CHILDS, C. (1995) Relay zone geometry
 529 and displacement transfer between normal faults recorded in coal-mine plans. *Journal*
 530 *of Structural Geology*, 17, 1741-1755.
- 531 JACKSON, C.A.L., ROTEVATN, A. (2013) 3D seismic analysis of the structure and
 532 evolution of a salt-influenced normal fault zone: a test of competing fault growth
 533 models. *Journal of Structural Geology*, 54, 215-234.
- 534 JACKSON, C.A.L., BELL, R.E., ROTEVATN, A., TVEDT, A.B. (2017) Techniques to
 535 determine the kinematics of synsedimentary normal faults and implications for fault
 536 growth models. In Childs, C., Holdsworth, R.E., Jackson, C.A.L., Manzocchi, T., Walsh,
 537 J.J., Yielding, G. (eds) *The Geometry and Growth of Normal Faults. Geological Society,*
 538 *London, Special Publications*, 439, 187-217.
- 539 JANKOWSKI, L., PROBULSKI, J. (2011) Tectonic and basinal evolution of the Outer
 540 Carpathians based on example of geological structure of the Grabownica, Strachocina
 541 and Łodyna hydrocarbon deposits. *Geologia*, 37, 555-583.

- 542 KATTENHORN, S.A., AYDIN, A. AND POLLARD, D.D. (2000) Joints at high angles to
543 normal fault strike: an explanation using 3-D numerical models of fault-perturbed stress
544 fields. *Journal of Structural Geology*, 22, 1-23.
- 545 KELLY, P.G., MCGURK, A., PEACOCK, D.C.P., SANDERSON, D.J. (1999) Reactivated
546 normal faults in the Mesozoic of the Somerset coast, and the role of fault scale in
547 reactivation. *Journal of Structural Geology*, 21, 493-509.
- 548 KIM, J.H. (1996) Mesozoic tectonics in Korea. *Journal of Southeast Asian Earth Sciences* 13,
549 251-265.
- 550 KRISTENSEN, T. B., ROTEVATN, A. , MARVIK, M. , HENSTRA, G. A., GAWTHORPE,
551 R. L. AND RAVNÅS, R. (2018) Structural evolution of sheared margin basins: the role
552 of strain partitioning. Sørvestsnaget Basin, Norwegian Barents Sea. *Basin Research*, 30,
553 279-301.
- 554 LAKE, S.D., KARNER, G.D. (1987) The structure and evolution of the Wessex Basin,
555 southern England: an examples of inversion tectonics. *Tectonophysics*, 137, 347-378.
- 556 LARSEN, P-H., (1988) Relay structures in a Lower Permian basement-involved extension
557 system, East Greenland. *Journal of Structural Geology*, 10, 3-8.
- 558 LONG, J.J. AND IMBER, J. (2011) Geological controls on fault relay zone scaling. *Journal*
559 *of Structural Geology*, 33, 1790-1800.
- 560 MANSFIELD, C. AND CARTWRIGHT, J. (2001) Fault growth by linkage: observations and
561 implications from analogue models. *Journal of Structural Geology*, 23, 745-763.
- 562 MCCLAY, K.R. (1989). Analogue models of inversion tectonics. In Cooper, M.A., Williams,
563 G.D. (eds) Inversion Tectonics. *Geological Society, London, Special Publications*, 44,
564 41-59.
- 565 MCCLAY, K. AND BONORA, M. (2001) Analog models of restraining stepovers in strike-
566 slip fault systems. *AAPG Bulletin*, 85, 233-260.

- 567 MCCLAY, K.R., BUCHANAN, P.G. (1992) Thrust faults in inverted extensional basins. In
568 McClay, K.R., Thrust Tectonics, pp. 93-104. Springer, Dordrecht.
- 569 MORLEY, C. K. (1995) Developments in the structural geology of rifts over the last decade
570 and their impact on hydrocarbon exploration. In: Lambiase, J.J. (ed.), Hydrocarbon
571 Habitat in Rift Basins. *Geological Society Special Publication*, 80, 1-32.
- 572 MORLEY, C.K., BACK, S., VAN RENSBERGEN, P., CREVELLO, P., LAMBIASE, J.J.
573 (2003) Characteristics of repeated, detached, Miocene–Pliocene tectonic inversion
574 events, in a large delta province on an active margin, Brunei Darussalam, Borneo.
575 *Journal of Structural Geology*, 25, 1147-1169.
- 576 MORLEY, C.K., NELSON, R.A., PATTON, T.L., MUNN, S.G. (1990) Transfer zones in the
577 East African rift system and their relevance to hydrocarbon exploration in rifts. *AAPG*
578 *Bulletin*, 74, 1234-1253.
- 579 PANIEN, M., SCHREURS, G., PFIFFNER, A. (2005) Sandbox experiments on basin
580 inversion: testing the influence of basin orientation and basin fill. *Journal of Structural*
581 *Geology*, 27, 433-445.
- 582 PEACOCK, D.C.P. (2002) Propagation, interaction and linkage in normal fault systems.
583 *Earth-Science Reviews*, 58, 121-142.
- 584 PEACOCK, D.C.P., KNIPE, R.J. AND SANDERSON, D.J. (2000) Glossary of normal faults.
585 *Journal of Structural Geology*, 22(3), pp.291-305.
- 586 PEACOCK, D.C.P., NIXON, C.W., ROTEVATN, A., SANDERSON, D.J., ZULUAGA, L.F.
587 (2016) Glossary of fault and other fracture networks. *Journal of Structural Geology*, 92,
588 12-29.
- 589 PEACOCK, D.C.P., NIXON, C.W., ROTEVATN, A., SANDERSON, D.J. AND
590 ZULUAGA, L.F. (2017) Interacting faults. *Journal of Structural Geology*, 97, pp.1-22.

- 591 PEACOCK, D.C.P., SANDERSON, D.J. (1991) Displacements, segment linkage and relay
592 zones in normal fault zones. *Journal of Structural Geology* 13, 721-733.
- 593 PEACOCK, D.C.P., SANDERSON, D.J. (1994) Geometry and development of relay zones in
594 normal fault systems. *AAPG Bulletin*, 78, 147-165.
- 595 PEACOCK, D.C.P., SANDERSON, D.J. (1995) Pull-aparts, shear fractures and pressure
596 solution. *Tectonophysics*, 241, 1-13.
- 597 PEACOCK, D.C.P., SANDERSON, D.J. (1999) Deformation history and basin-controlling
598 faults in the Mesozoic sedimentary rocks of the Somerset coast. *Proceedings of the*
599 *Geologists Association*, 110, 41-52.
- 600 PEACOCK, D.C.P., SHEPHERD, J. (1997) Reactivated faults and transfer zones in the
601 Southern Coalfield, Sydney Basin, Australia, *Australian Journal of Earth Sciences* 44,
602 265-273.
- 603 PEACOCK, D.C.P., KNIPE, R.J., SANDERSON, D.J. (2000) Glossary of normal faults.
604 *Journal of Structural Geology*, 22, 291-305.
- 605 RAWNSLEY, K.D., PEACOCK, D.C.P., RIVES, T., PETIT, J.-P. (1998) Jointing in the
606 Mesozoic sediments around the Bristol Channel Basin. *Journal of Structural Geology*,
607 20, 1641-1661.
- 608 RICHARD, P., KRANTZ, R.W. (1991) Experiments on fault reactivation in strike-slip mode.
609 *Tectonophysics*, 188, 117-131.
- 610 ROBERTS, D.G. (1989) Basin inversion in and around the British Isles. Cooper, M.A.,
611 Williams, G.D. (eds) *Inversion Tectonics. Geological Society, London, Special*
612 *Publications*, 44, 131-150.
- 613 ROWLAND, J.V. AND SIBSON, R.H. (2004) Structural controls on hydrothermal flow in a
614 segmented rift system, Taupo Volcanic Zone, New Zealand. *Geofluids*, 4(4), pp.259-
615 283.

- 616 ROTEVATN, A., BASTESEN, E. (2014) Fault linkage and damage zone architecture in tight
617 carbonate rocks in the Suez Rift (Egypt): implications for permeability structure along
618 segmented normal faults. In Spence, G.H., Redfern, J., Aguilera, R., Bevan, T.G.,
619 Cosgrove, J.W., Couples, G.D., Daniel, J.M. (eds) *Advances in the Study of Fractured
620 Reservoirs. Geological Society, London, Special Publications*, 374, 79-95.
- 621 ROTEVATN, A., JACKSON, C.A.L. (2014) 3D structure and evolution of folds during
622 normal fault dip linkage. *Journal of the Geological Society, London*, 171, 821-829.
- 623 ROTEVATN, A., FOSSEN, H., HESTHAMMER, J., AAS, T.E., HOWELL, J.A. (2007) Are
624 relay zones conduits for fluid flow? Structural analysis of a relay zone in Arches
625 National Park, Utah. In Lonergan, L., Jolly, R.J.H., Rawnsley, K., Sanderson, D.J. (eds)
626 *Fractured Reservoirs. Geological Society, London, Special Publications*, 270, 55-71.
- 627 ROTEVATN, A., TVERANGER, J., HOWELL, J.A., FOSSEN, H. (2009) Dynamic
628 investigation of the effect of a relay zone on simulated fluid flow: geocellular modelling
629 of the Delicate Arch Ramp, Utah. *Petroleum Geoscience*, 15, 45-58.
- 630 SCOTese, C.R. (1991) Jurassic and Cretaceous plate tectonic reconstructions.
631 *Palaeogeography, Palaeoclimatology, Palaeoecology* 87, 493-501.
- 632 SOLIVA, R., BENEDICTO, A. (2004) A linkage criterion for segmented normal faults.
633 *Journal of Structural Geology*, 26, 2251-2267.
- 634 SYLVESTER, A.G. (1988) Strike-slip faults. *Geological Society of America Bulletin*, 100,
635 1666-1703.
- 636 TAPPIN, D.R., CHADWICK, R.A., JACKSON, A.A., WINGFIELD, R.T.D., SMITH, N.J.P.
637 (1994) The Geology of Cardigan Bay and the Bristol Channel. *British Geological
638 Survey, United Kingdom Offshore Report*.

- 639 TAVANI, S., MENCOS, J., BAUSÀ, J., MUÑOZ, J.A. (2011) The fracture pattern of the
640 Sant Corneli Bóixols oblique inversion anticline (Spanish Pyrenees). *Journal of*
641 *Structural Geology*, 33, 1662-1680.
- 642 TURNER, S.A., LIU, J.G., COSGROVE, J.W. (2011) Structural evolution of the Piqiang
643 Fault Zone, NW Tarim Basin, China. *Journal of Asian Earth Sciences*, 40, 394-402.
- 644 VAN HOORN, B. (1987). The south Celtic Sea/Bristol Channel basin: origin, deformation
645 and inversion history. *Tectonophysics*, 137, 309-334.
- 646 VAN NOTEN, K., CLAES, H., SOETE, J., FOUBERT, A., ÖZKUL, M., SWENNEN, R.
647 (2013) Fracture networks and strike-slip deformation along reactivated normal faults in
648 Quaternary travertine deposits, Denizli Basin, western Turkey. *Tectonophysics*, 588,
649 154-170.
- 650 WALSH, J.J., BAILEY, W.R., CHILDS, C., NICOL, A. AND BONSON, C.G. (2003)
651 Formation of segmented normal faults: a 3-D perspective. *Journal of Structural*
652 *Geology*, 25, 1251-1262.
- 653 WALSH, J.J., NICOL, A. AND CHILDS, C. (2002) An alternative model for the growth of
654 faults. *Journal of Structural Geology*, 24, 1669-1675.
- 655 WALSH, J. J., WATTERSON, J. (1987). Distributions of cumulative displacement and
656 seismic slip on a single normal fault. *Journal of Structural Geology*, 9, 1039-1046.
- 657 WHITTAKER, A., GREEN, G.W. (1983). Geology of the Country Around Weston-super-
658 Mare. *Memoir of the Geological Survey of Great Britain*, Sheet 279 and parts of 263
659 and 295.
- 660 WILLIAMS, G.D., POWELL, C.M., COOPER, M.A. (1989). Geometry and kinematics of
661 inversion tectonics. In: Cooper, M.A., Williams, G.D. (eds.), *Inversion Tectonics*.
662 *Geological Society Special Publication*, 44, 3-15.

- WONG, V., MUNGUÍA, L. (2006). Seismicity, focal mechanisms, and stress distribution in the Tres Vírgenes volcanic and geothermal region, Baja California Sur, Mexico. *Geofísica internacional*, 45, 23-37.
- XU, S., NIETO-SAMANIEGO, Á.F., ALANIZ-ÁLVAREZ, S.A., CERCA-MARTÍNEZ, L.M. (2011) Structural analysis of a relay zone in the Querétaro graben, central Mexico: implications for relay zone development. *Revista mexicana de ciencias geológicas*, 28, 275-289.
- YAMADA, Y., MCCLAY, K. (2004) 3-D analog modeling of inversion thrust structures. In: McClay, K. (eds.), Thrust Tectonics and Hydrocarbon Systems. *AAPG Memoir* 82, 276-301.
- ZAMPIERI, D., MASSIRONI, M. (2007) Evolution of a poly-deformed relay zone between fault segments in the eastern Southern Alps, Italy. In: Cunningham, W.D., Mann, P. (eds) Tectonics of Strike-Slip Restraining and Releasing Bends. *Geological Society, London, Special Publications*, 290, 351-366.

Figure captions

Fig. 1. Schematic diagrams of the main map-view fault geometries described in this paper. (a) A *transfer zone* between two stepping sub-parallel normal faults of any relative dip direction (e.g. Morley et al., 1990). (b) A *relay ramp*, between two stepping sub-parallel normal faults with the same dip direction (e.g. Larsen, 1988). (c) A *breached relay*, where the stepping faults are linked by a *connecting fault* (e.g. Peacock & Sanderson, 1991). (d) A *contractional step* between two right-stepping sinistral faults. (e) An *extensional step* between two left-stepping sinistral faults. (f) A relay ramp reactivated as a contractional step.

Fig. 2. Geological map of Somerset, the Bristol Channel Basin and surrounding areas. The location of the study area at Lilstock is shown. From Engelder and Peacock (2001).

Fig. 3. (a) Map of the reactivated normal fault zone at Lilstock, Somerset. Segments B through D are shown; Segment A falls outside the area shown in this image but is poorly exposed. Lower hemisphere stereonet show the orientation of (i) beds at distance from the fault zone, (ii) beds within the relay zones, (iii) normal faults reactivated as sinistral strike-slip faults, and (iv) normal faults elsewhere in the broader study area (mostly outside the area shown in this figure) that are not reactivated by strike-slip reactivation. (b) One of the reactivated relay ramps along the fault system shown in (a). The location is shown in (a). Both figures were made using merged images taken from a UAV.

Fig. 4. Field photographs showing evidence for strike-slip reactivation of the fault zone at Lilstock. (a) View westwards along the fault showing steepened relay zones. (b) Close-up view towards the west showing the steepened beds of one of the relay zones. (c) E-W striking left-stepping calcite veins linked to form a sinistral strike-slip fault in the east of the fault zone. (d) Slickenside lineations with evidence of strike-slip dominated (sinistral) displacement during reactivation. (e) Folding and thrusting in the footwall of a normal fault in the east of the fault zone (view towards the west). (f) Crenulation cleavage in shale in a fold in the east of the fault zone. The locations of (a) and (b) are shown in Figure 3b. The photographs showing structural detail (c), (e) and (f) were taken within and around the reactivated relay zone shown in Figure 3b. Photograph (d) was taken along Segment D, which is shown in Figure 3a.

Fig. 5. Field photograph of a south-dipping normal faults and associated E-W striking calcite veins, exposed in the eastern part of the fault zone at Lilstock. These structures indicate initial ~ N-S extension.

Fig. 6. Schematic figure showing the effects of strike-slip reactivation on normal fault zones.

Fig. 7. A km-scale normal fault system reactivated as a sinistral-strike slip fault in the Italian Alps (from Zampieri & Massironi, 2007). Note the (originally extensional) transfer zone to the south, between the Garmonda and Tormeno faults, which has been reactivated as a restraining stepover. See text for full discussion. Note also the releasing stepover to the north, between the Tormeno and Melegnon faults.

Fig. 8. (a) The Sulaiman-Kirthar arcuate fold and thrust belt in Pakistan. This originated as a 100s-km-scale extensional transfer zone in a Mesozoic rift system between Africa, Madagascar and India, but underwent sinistral reactivation in Eocene times during the collision between the Indian and Eurasian plates, leading the transfer zone to turn into an arcuate fold and thrust belt. (b) Schematic figure illustrating the deformation in the Sulaiman-Kirthar ranges.

Fig. 9. Relay length (fault overlap) vs relay width (fault separation) of the inverted relay zones this study plotted with global data from previous studies. The figure is modified from Fossen & Rotevatn (2016), and the global data are from the same paper and from Mansfield & Cartwright (2001), Long & Imber (2011). F&R16 = Fossen & Rotevatn (2016). Note that the data from the example shown in Fig. 3 ($n = 4$) plot well within the cloud of points that defines the global trend.

738

739 **Fig. 10.** Distribution of maximum dip of relay zones that are: (a) unbreached; (b) partly
740 breached; (c) strongly breached, and; (d) inverted. The data in (a), (b) and (c) are derived from
741 outcrop examples from Soliva & Benedicto (2004); Huggins et al. (1995); Xu et al. (2011);
742 Rotevatn & Bastesen (2012); Giba et al. (2012), and Bastesen & Rotevatn (2012). Dip is
743 relative to the general (regional) layer orientation. (a), (b) and (c) are modified from Fossen &
744 Rotevatn (2016), whereas (d) presents data from this study.

745

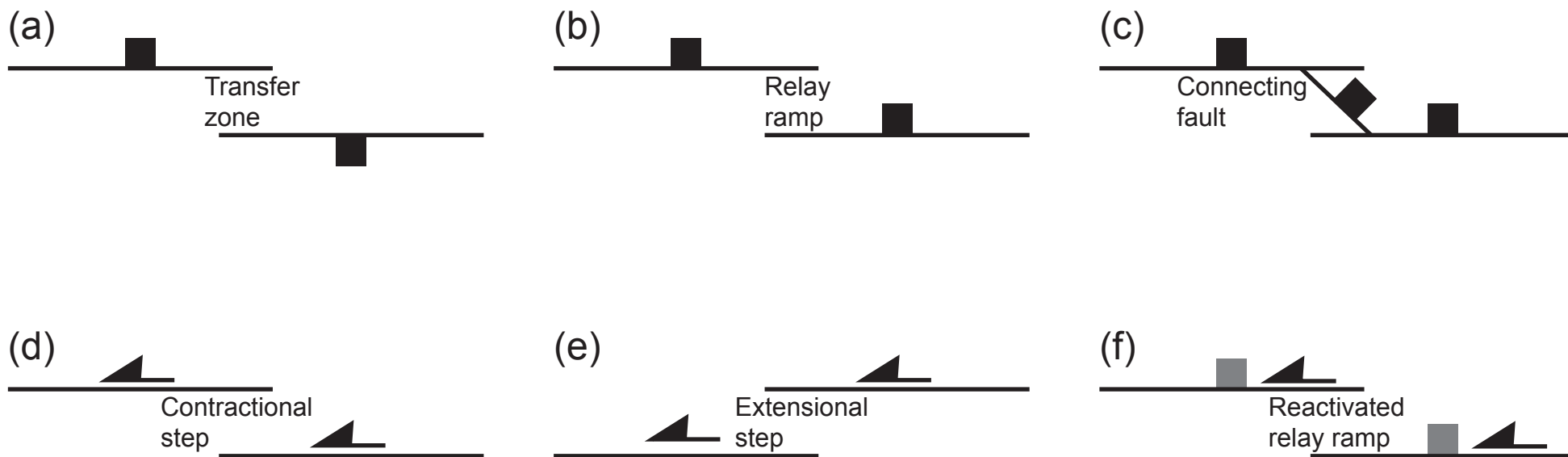


Figure 1

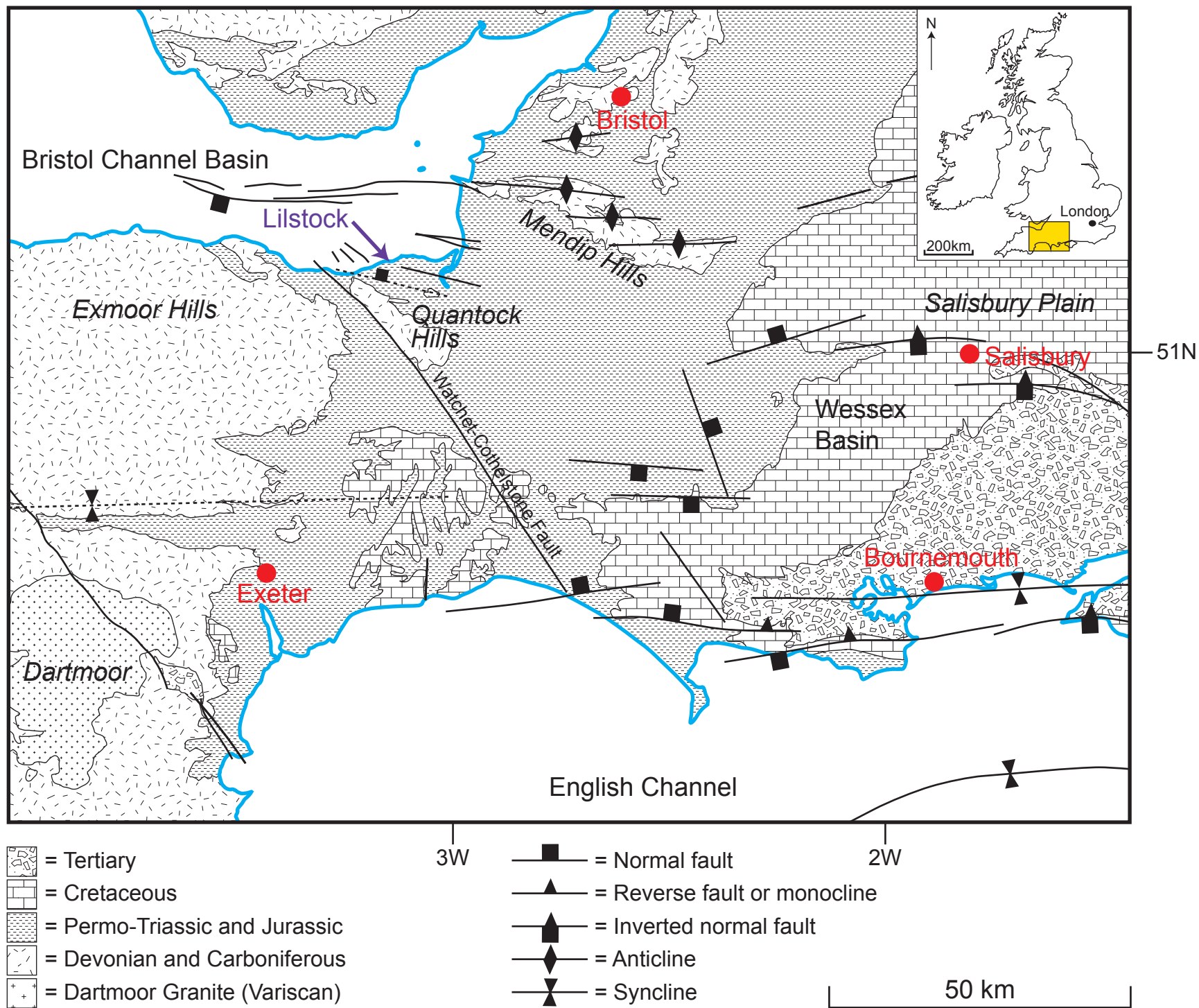


Figure 2

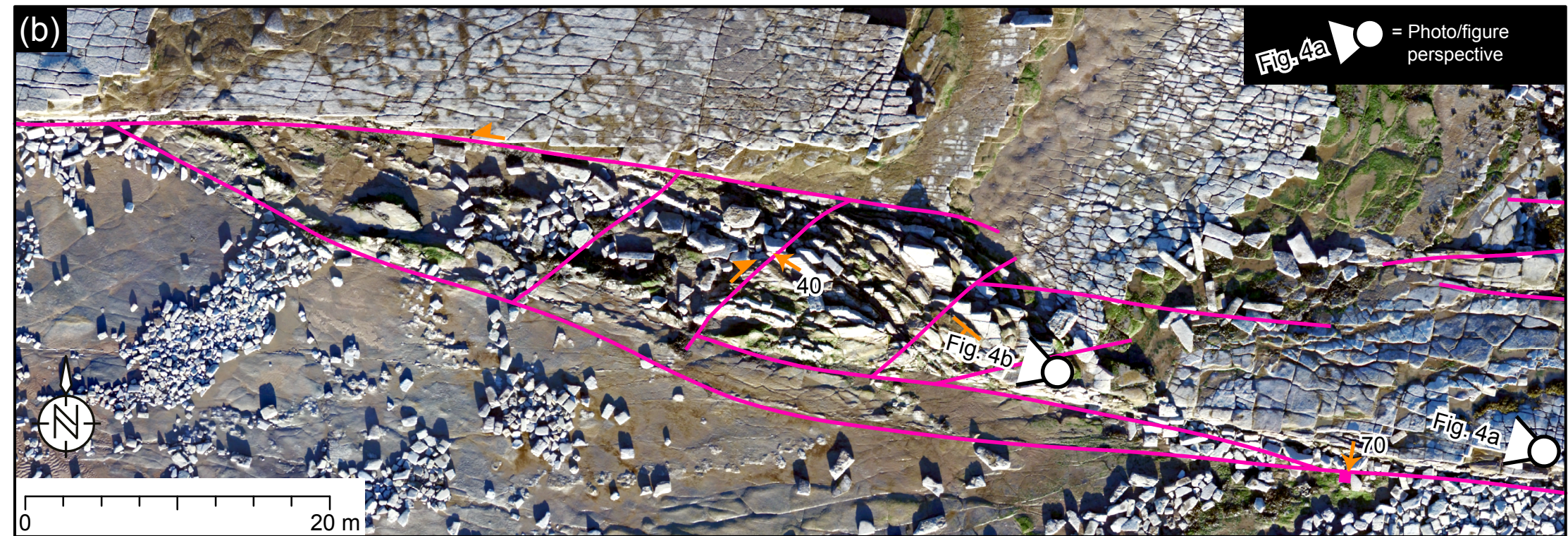
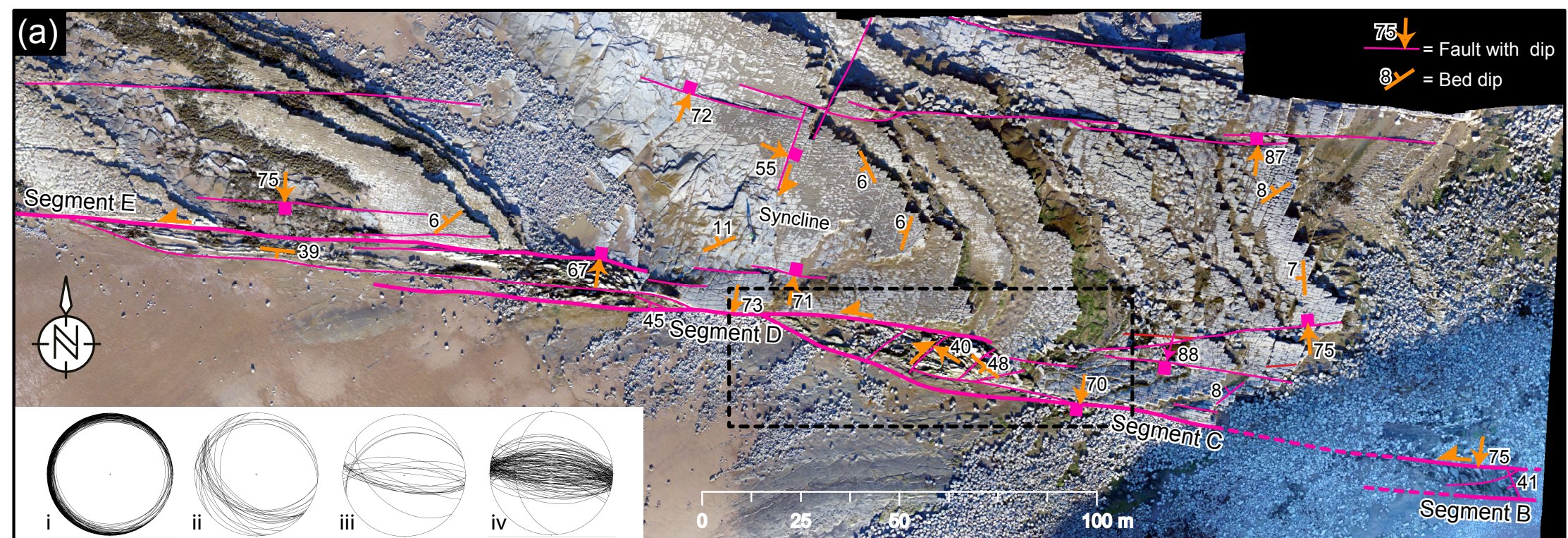


Figure 3

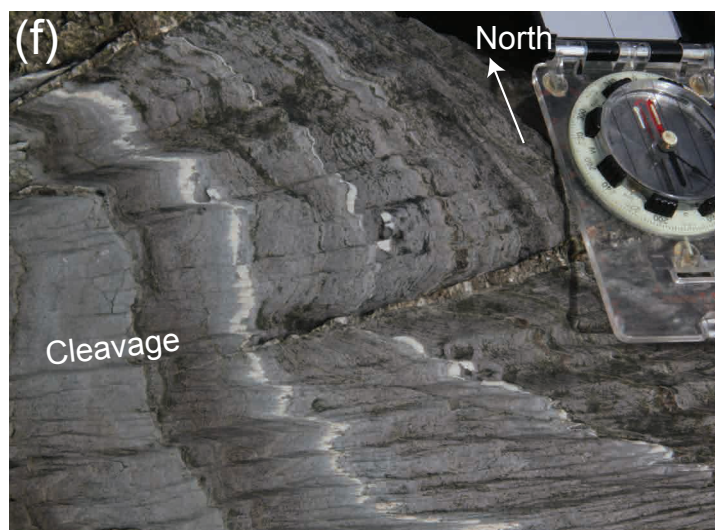
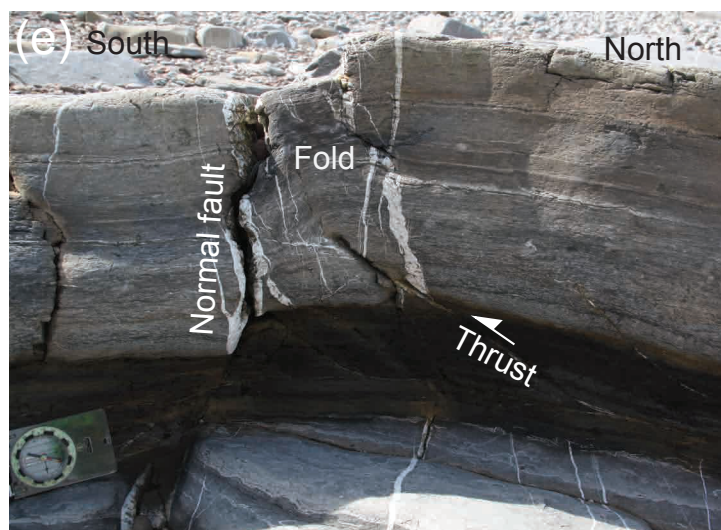
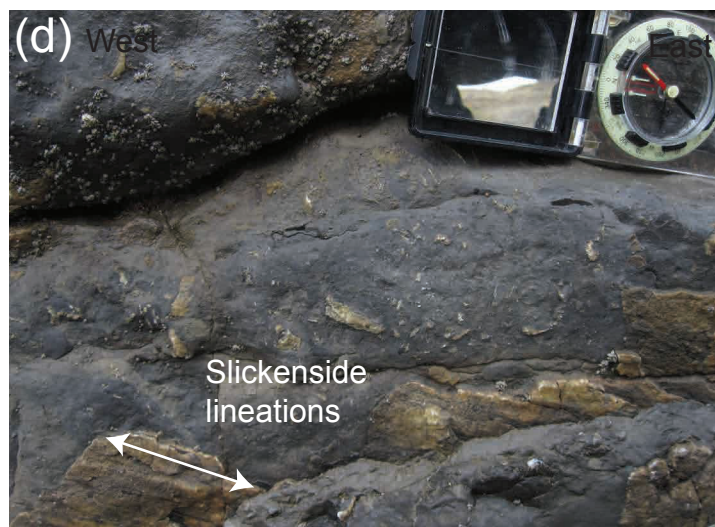
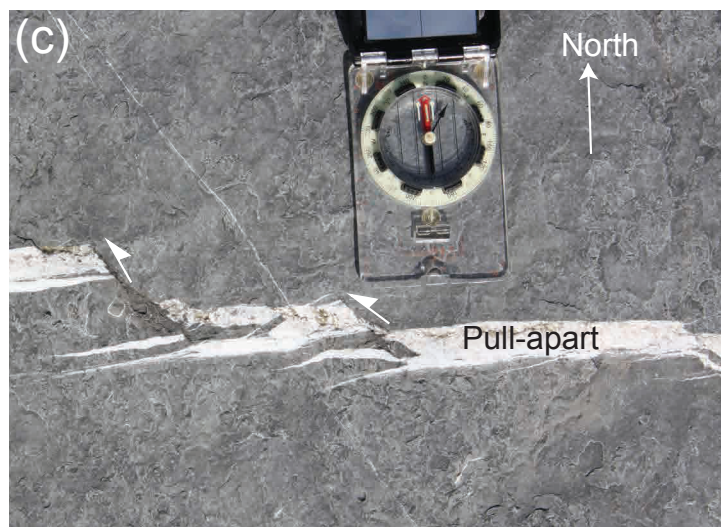
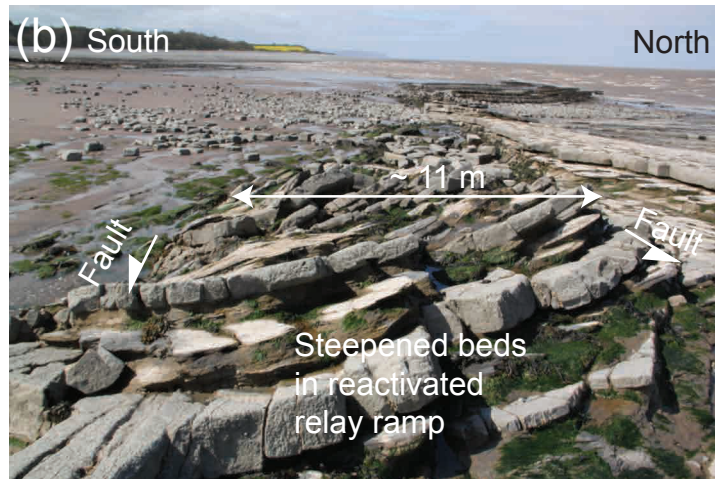


Figure 4



Figure 5

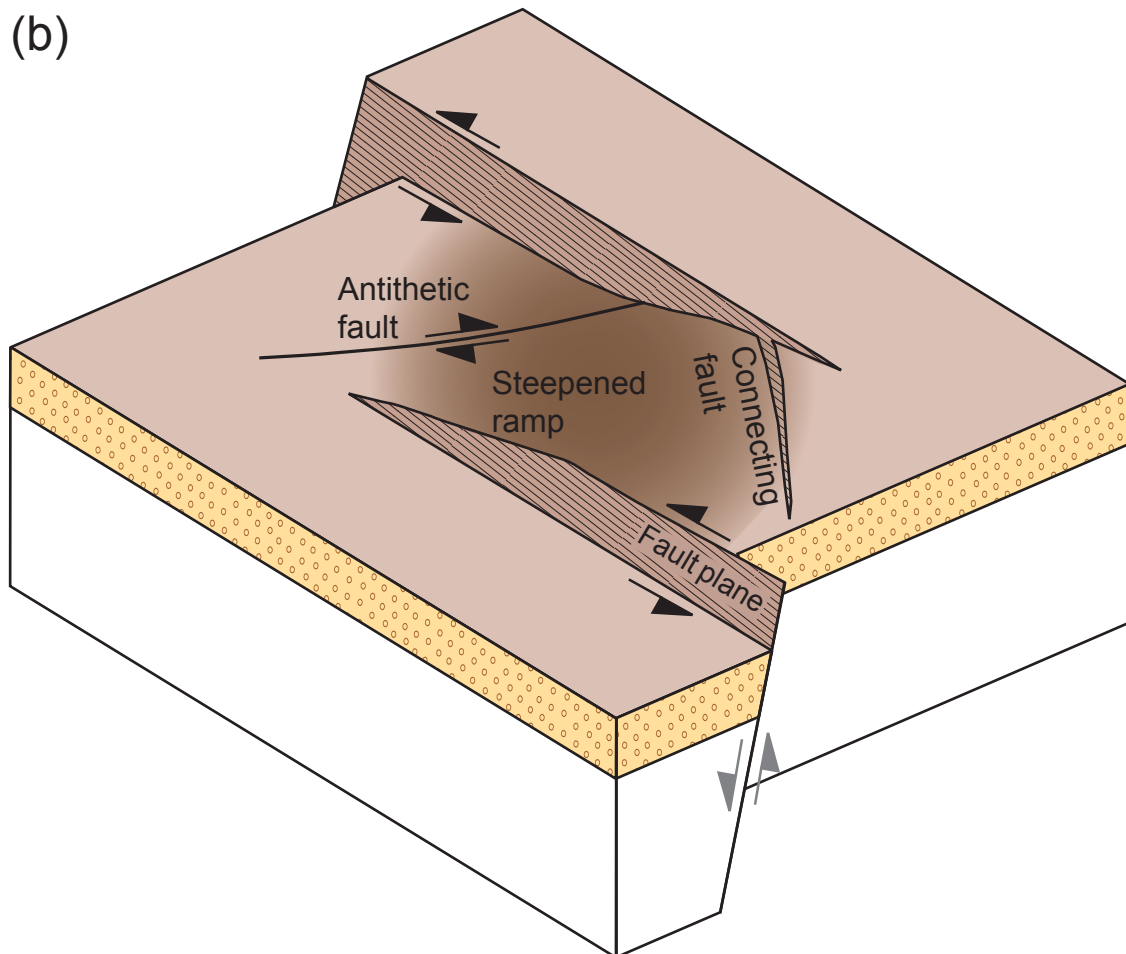
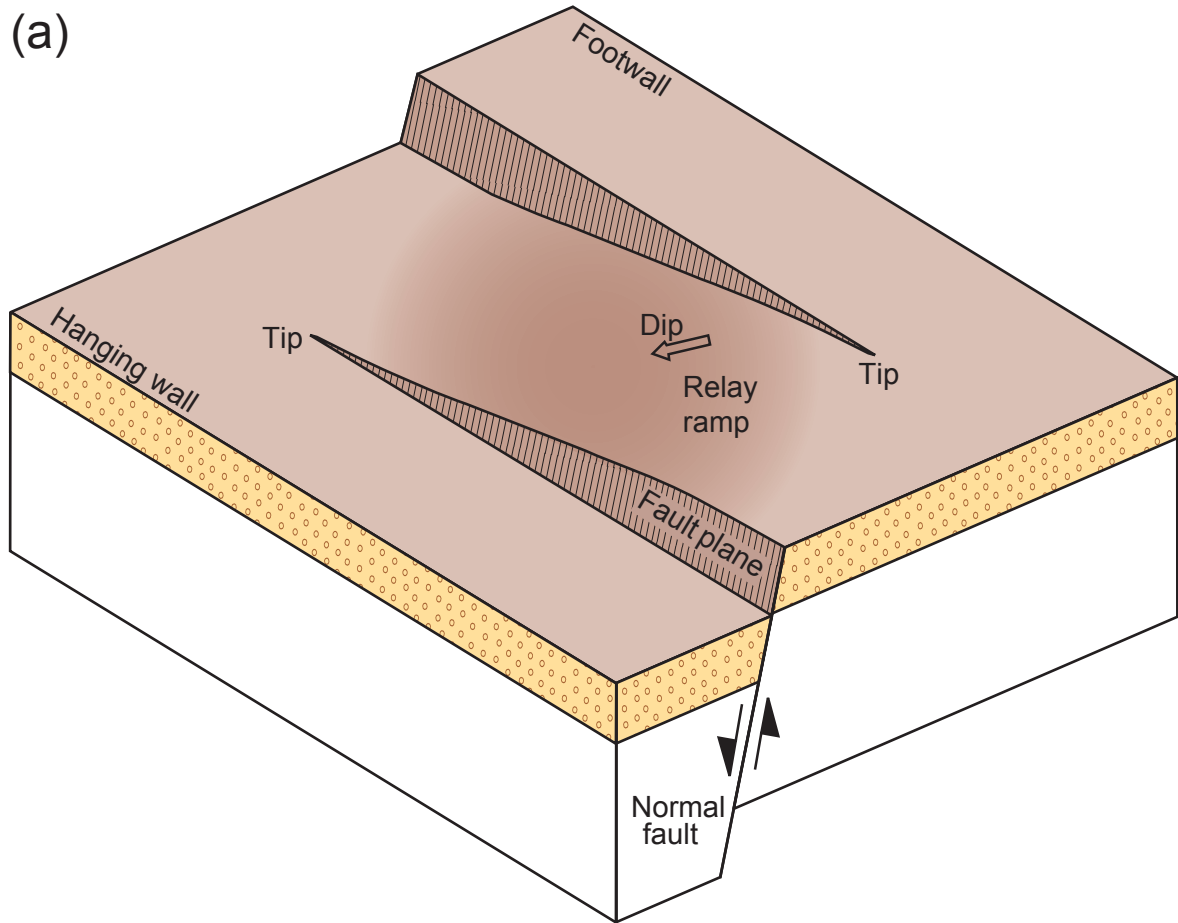
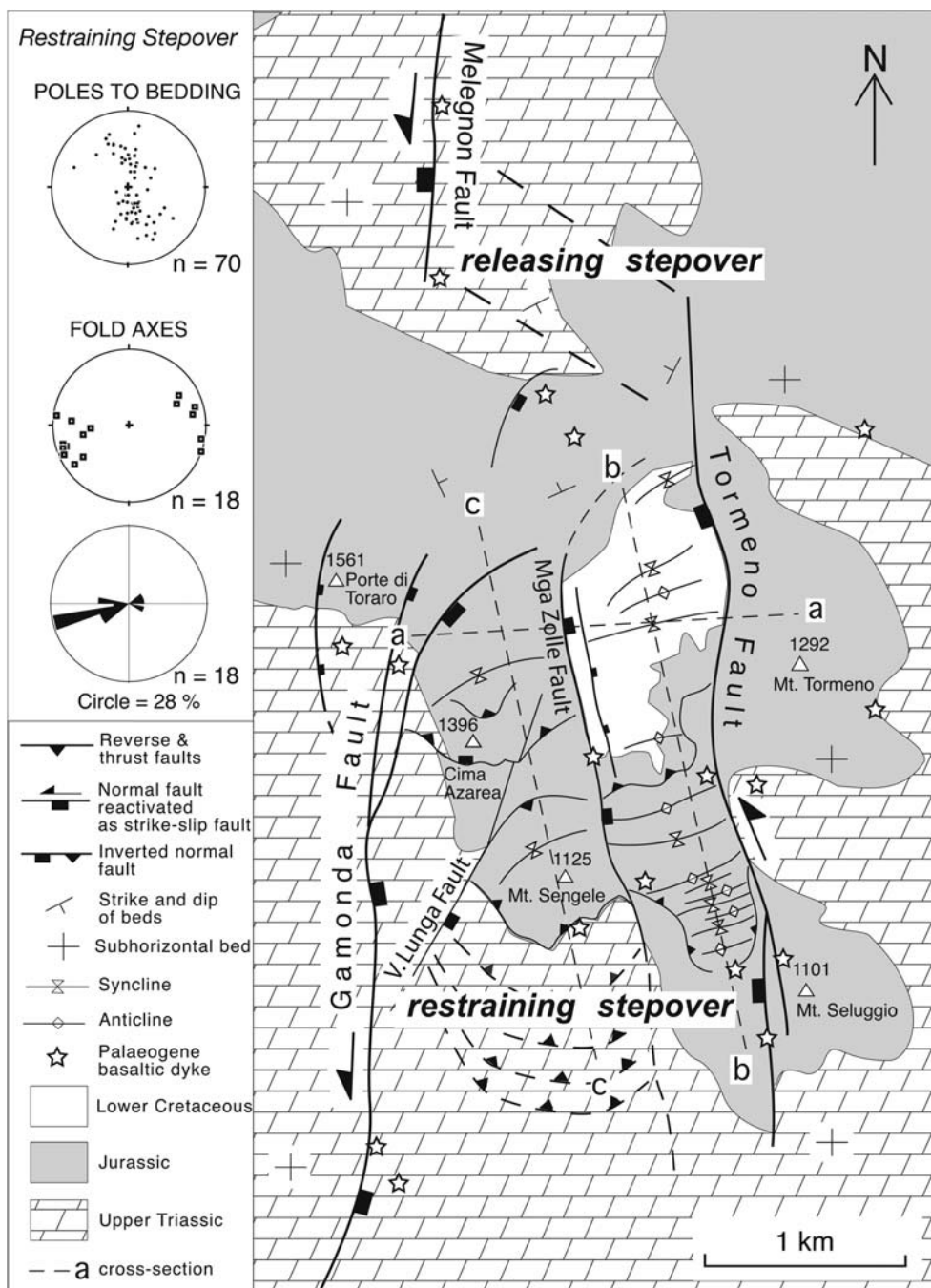


Figure 6



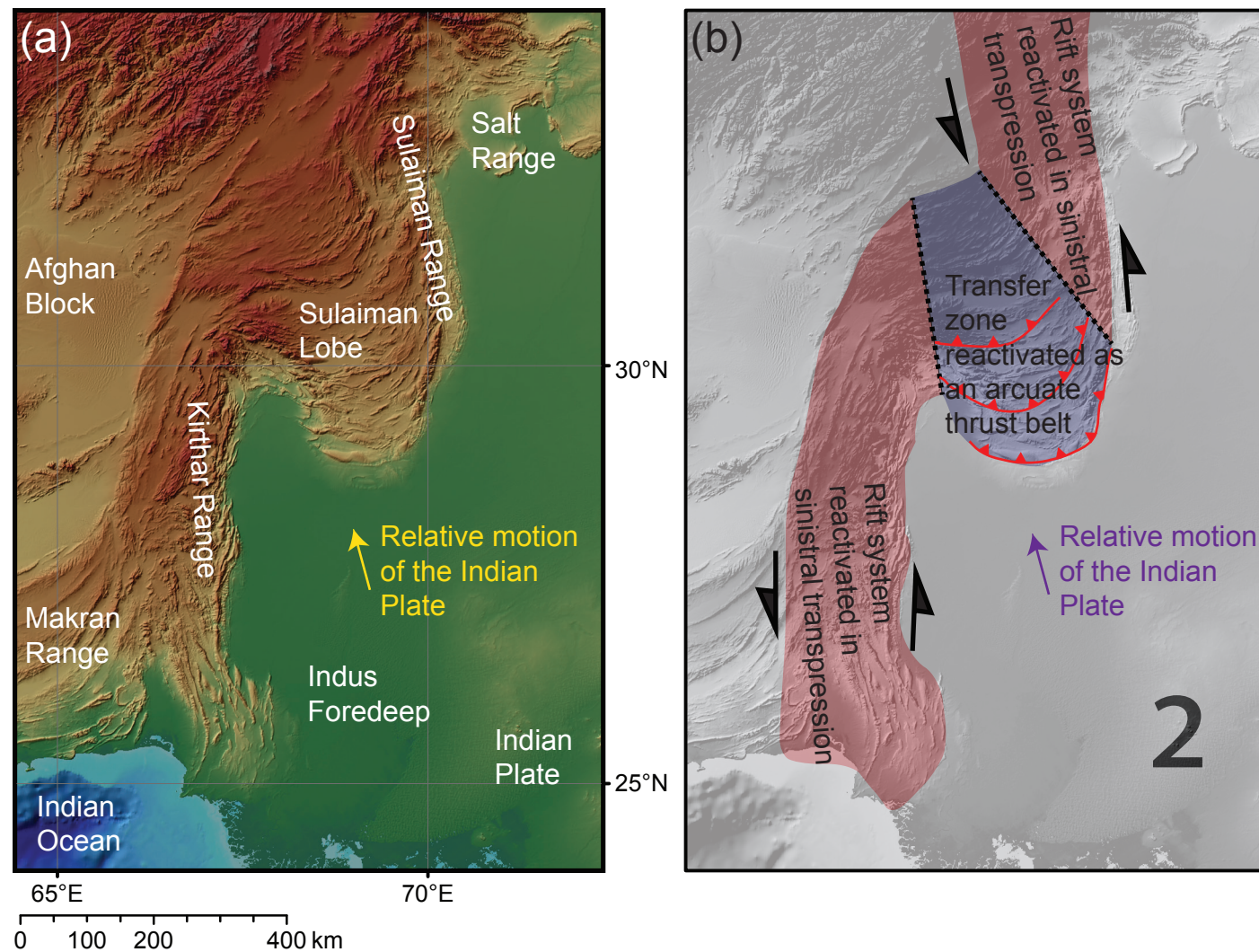


Figure 8

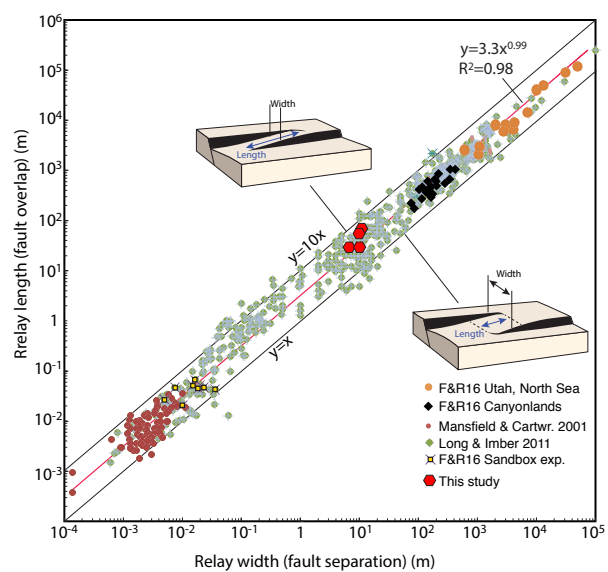


Figure 9

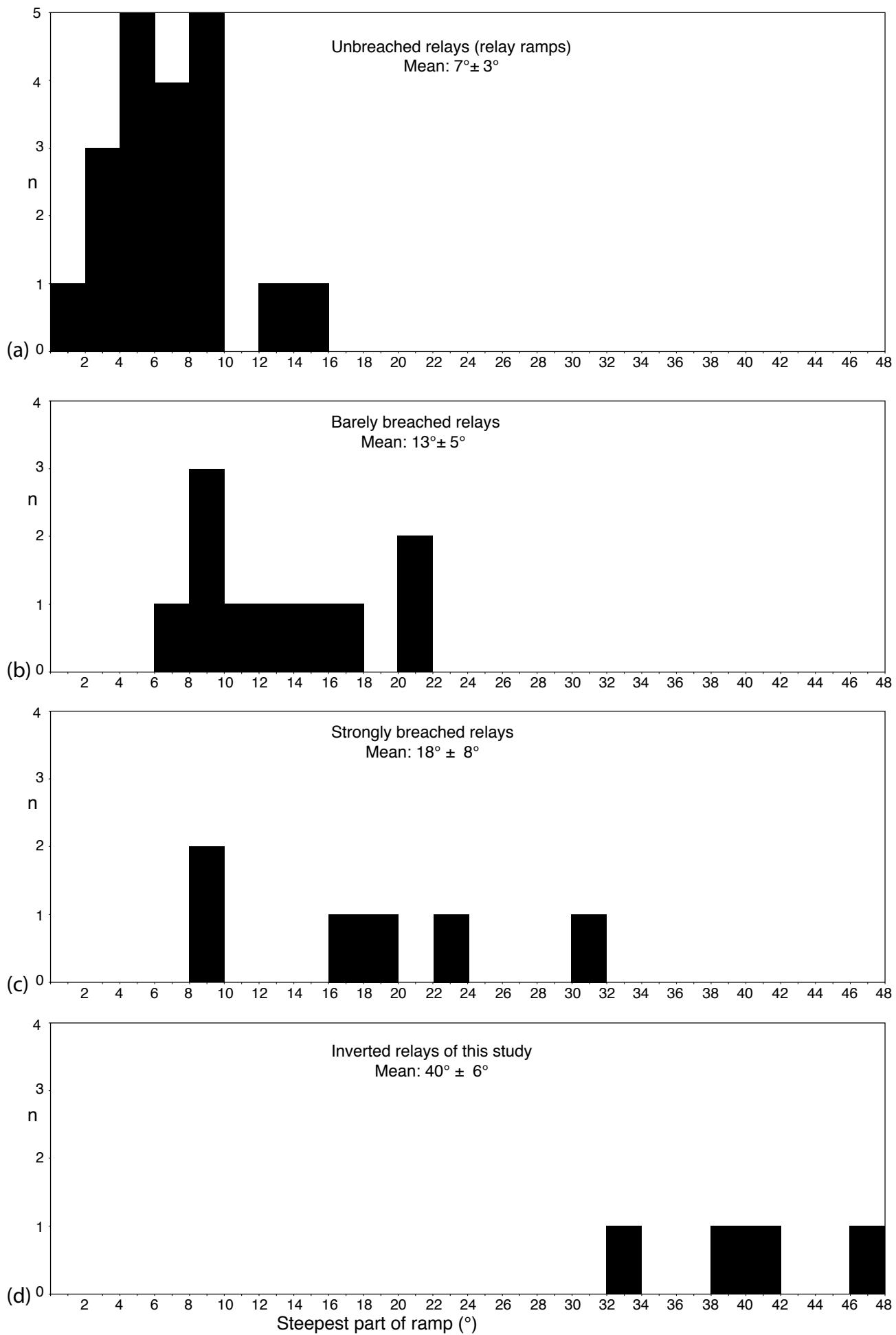


Figure 10